
REGRET-BASED FEDERATED CAUSAL DISCOVERY WITH UNKNOWN INTERVENTIONS

A PREPRINT

Federico Baldo¹ and Charles K. Assaad¹

¹Sorbonne Université, INSERM, Institut Pierre Louis d’Epidémiologie et de Santé Publique, F75012, Paris, France

ABSTRACT

Most causal discovery methods recover a completed partially directed acyclic graph representing a Markov equivalence class from observational data. Recent work has extended these methods to federated settings to address data decentralization and privacy constraints, but often under idealized assumptions that all clients share the same causal model. Such assumptions are unrealistic in practice, as client-specific policies or protocols, for example, across hospitals, naturally induce heterogeneous and unknown interventions. In this work, we address federated causal discovery under unknown client-level interventions. We propose I-PERI, a novel federated algorithm that first recovers the CPDAG of the union of client graphs and then orients additional edges by exploiting structural differences induced by interventions across clients. This yields a tighter equivalence class, which we call the Φ -Markov Equivalence Class, represented by the Φ -CPDAG. We provide theoretical guarantees on the convergence of I-PERI, as well as on its privacy-preserving properties, and present empirical evaluations on synthetic data demonstrating the effectiveness of the proposed algorithm.

1 Introduction

Discovering causal structures from observational and interventional data is a challenging task at the core of many scientific disciplines. Indeed, recovering causal relationships among variables is key to causal effect estimation, as it allows for the identification of confounding variables Pearl (2009); Spirtes et al. (2001); Hernan & Robins (2023). Many causal discovery algorithms (Spirtes et al., 2001; Colombo & Maathuis, 2014; Runge, 2020; Assaad et al., 2022) aim to recover, from observational data, a completed partially directed acyclic graph (CPDAG) (Chickering, 2003), which represents the Markov equivalence class (Verma & Pearl, 1990) of an underlying causal graph. These methods typically assume access to a centralized dataset. In many real-world scenarios, however, data are inherently decentralized and cannot be pooled due to practical or legal constraints. This has motivated growing interest in federated learning Kairouz et al. (2021), where data are distributed across multiple clients, for example, hospitals, institutions, or organizations, each of which holds its own local dataset. A central server coordinates the learning process by aggregating information communicated by the clients, without accessing their individual datasets.

Beyond decentralization, federated approaches are particularly appealing in domains where data sharing is restricted by regulatory requirements, data ownership constraints, or privacy concerns. However, the challenge of designing privacy-preserving federated causal discovery algorithms has been largely overlooked in many existing works. Recent works (Mian et al., 2022, 2023; Li et al., 2023) have addressed these challenges in an idealized setting, where all clients’ data are assumed to be generated from the same underlying causal model, with no interventions, and thus share an identical causal graph. This assumption is frequently unrealistic in real-world applications. For instance, in healthcare scenarios, different hospitals may adopt distinct treatment policies, diagnostic protocols, or patient inclusion criteria. These differences naturally induce client-specific interventions and lead to heterogeneous causal mechanisms.

In this paper, we study the problem of federated causal discovery under unknown client-level interventions. We propose I-PERI, a novel federated causal discovery algorithm capable of handling unknown interventions at the client level while ensuring differential privacy. I-PERI is an extension of the recently proposed PERI algorithm Mian et al. (2023); this method assumes that all clients share the same causal structure, and it is capable of discovering the CPDAG

common to all clients from purely observational data in a differentially private fashion. I-PERI extends PERI to leverage interventional data by introducing a two-phase approach: first, it learns the CPDAG corresponding to the union of all client causal graphs by adapting PERI algorithm to interventional data; then, it refines the learned structure by orienting additional edges, exploiting structural differences induced by interventions across clients. More specifically, our contributions are threefold:

- We introduce the Φ -Markov Equivalence Class of DAGs under a set of unknown interventions in a federated setting, which forms a tighter equivalence class than the standard Markov equivalence class, along with a representative graph for this class, the Φ -CPDAG.
- We propose I-PERI, a novel algorithm for federated causal discovery that effectively combines observational and interventional data from multiple clients while ensuring differential privacy and without knowing the interventional targets.
- We provide theoretical guarantees on the convergence of I-PERI, as well as on its privacy-preserving properties, and present empirical evaluations on synthetic data demonstrating the effectiveness of the proposed algorithm.

The remainder of this paper is organized as follows. Section 2 introduces the necessary background and preliminaries. Section 3 presents the proposed framework and algorithm. Section 4 provides experimental results and empirical evaluations. Finally, Section 5 concludes the paper and discusses future directions.

2 Preliminaries & Problem Setup

In this section, we introduce the notations and concepts used throughout the paper, outline the problem, and present key methodological insights.

Causal Graphs. A causal directed acyclic graph (DAG) is a graphical representation of causal relationships between random variables. More formally, $G = (\mathbb{V}, \mathbb{E})$ is a DAG where $\mathbb{V} = V_1, V_2, \dots, V_d$ is the set of nodes representing random variables and $\mathbb{E} \subseteq \mathbb{V} \times \mathbb{V}$ is the set of directed edges representing direct causal relationships between the variables. We denote with P_\emptyset the joint probability distribution over \mathbb{V} that factorizes according to the causal DAG G as follows:

$$P_\emptyset(\mathbb{V}) = \prod_i P_\emptyset(V_i | V_{pa_{V_i}^G})$$

where $pa_{V_i}^G$ are the parents of V_i in G . We also denote the skeleton of the graph, $Skel(G)$, as the unoriented version of the DAG, i.e., the graph obtained by removing the directionality of the edges. A key notion in DAGs is d-separation, denoted $\perp\!\!\!\perp_G$, which encodes the conditional independencies implied by the graph. *Causal discovery* aims at learning the causal DAG G or rather a partially oriented version of the DAG from data sampled from the joint distribution P_\emptyset . In general, a causal DAG or its partially oriented version cannot be discovered from observational data without additional assumptions. In this work, we adopt two standard assumptions commonly used in discovery methods. The first is the causal sufficiency assumption, which posits that all common causes of the observed variables are themselves observed, i.e., there are no latent confounders. The second is the faithfulness assumption, which states that all and only the conditional independencies present in the distribution P_\emptyset are implied by d-separation.

Federated causal discovery aims to learn a global graph at a central server, given a distributed setting. In this paper, we focus on federated algorithms that provide privacy-preserving guarantees by design, without relying on cryptographic techniques. For example, let us consider multiple hospitals conducting different clinical trials; in this context, we might want to learn a graph from the joint data while preserving patient privacy. We assume to have K clients, each holding a local dataset \mathbb{D}^k , for $k \in 1, \dots, K$. Each dataset involve the same set of variables $\mathbb{V} = V_1, \dots, V_d$, and may contain different numbers of samples, n^1, \dots, n^K . In most existing works, clients' data are assumed to be generated from the same underlying causal DAG G over \mathbb{V} , which is ideally the one we want to recover at the server level. This assumption is often unrealistic in practice. In our example, the different clinical trials might involve distinct treatment protocols, eligibility criteria, and intervention strategies. As a result, patient data are generated under hospital-specific interventions, leading to heterogeneous causal structures.

Interventions. The causal DAG, alongside the joint distribution P , allow us to describe interventions on the system. In the scope of this work, we consider *general interventions*, meaning that an intervention can be: either *parametric*, where the functional form of the conditional distribution of the intervened variable is changed, or *structural*, where the causal mechanism of the intervened variable is replaced, removing some or all incoming edges to the intervened node. Note that parametric interventions do not modify the causal DAG.

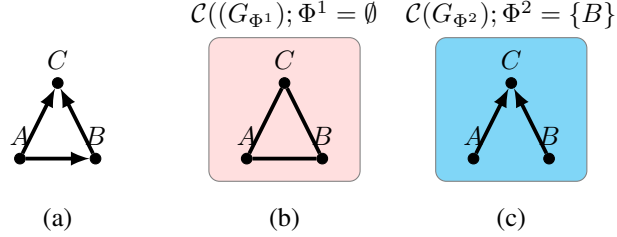


Figure 1: (a) True causal DAG; (b) Client CPDAG with no interventions; (c) Client CPDAG with interventions.

Definition 2.1 (General intervention). Under general interventions on a target set $\mathbb{I} \subseteq \mathbb{V}$, such that $\mathbb{I} = \mathbb{P} \cup \mathbb{S}$, where \mathbb{P} is the set of parametric interventions and \mathbb{S} the set of structural interventions, the post-intervention distribution $P_{\mathbb{I}}$ is given by:

$$P_{\mathbb{I}}(\mathbb{V}) = \prod_{V_i \in \mathbb{S}} P_{\mathbb{S}}(V_i | Pa_i^{G_{\mathbb{S}}}) \prod_{V_j \in \mathbb{P}} P_{\mathbb{P}}(V_j | Pa_j^G) \prod_{V_k \notin \mathbb{P} \cup \mathbb{S}} P_{\emptyset}(V_k | Pa_k^G).$$

For the remainder of this paper, we focus primarily on structural interventions, as they represent the most significant and challenging application scenario for our approach. Nevertheless, the algorithm introduced in this paper is sound even in the presence of parametric interventions or no interventions. For more details, see Section 5.

We now introduce the notion of a mutilated graph, which is a standard tool for representing interventions in causal models by modifying the underlying causal DAG.

Definition 2.2 (Mutilated graph). Let $G = (\mathbb{V}, \mathbb{E})$ be a causal DAG and $\mathbb{S} \subseteq \mathbb{V}$ be a set of structurally intervened variables. The mutilated graph, $G_{\mathbb{S}}$, is obtained by removing all or part of the incoming edges to the nodes in \mathbb{S} .

We emphasize that the mutilated graph $G_{\mathbb{S}}$ is a subgraph of in the original causal DAG G , i.e., $G_{\mathbb{S}} \subseteq G$. Moreover, unlike most definitions of mutilated graph in the literature, which assume that all incoming edges to an intervention target are removed, we adopt a more general notion in which only a subset of the incoming edges may be removed.

In the scope of this paper, we consider clients that may be subject to *unknown general interventions*. We denote a family of unknown interventions target for a set of clients as $\Phi = \Phi^1, \dots, \Phi^K$, where $\Phi^k \in \Phi$ represents a set of intervention targets for client k , $\Phi^k \subseteq \mathbb{V}$. This means that each client k may have their own distribution P_{Φ^k} under interventions Φ^k and mutilated causal DAG, G_{Φ^k} . Moreover, we assume that at least one client holds purely observational data, as stated in the following assumption.

Assumption 2.1. There exists $k \in 1, \dots, K$ such that $\Phi_k = \emptyset$.

Note that, unlike other methods assuming known interventions Hauser & Bühlmann (2012); Yang et al. (2018), we do not have access to the intervention targets across clients, since it could imply a privacy requirement violation, nor are we inferring the intervention targets Jaber et al. (2020); Li et al. (2023).

Greedy Equivalence Search. Among the different approaches for causal discovery, score-based methods estimate a graph \hat{G} that maximizes a given scoring criterion $S(H, \mathbb{D})$ over a dataset \mathbb{D} :

$$\hat{G} = \arg \max_{H \in \mathbb{G}} S(H, \mathbb{D})$$

where the search is performed over the space of all the possible CPDAGs \mathbb{G} . A popular score-based method is the Greedy Equivalence Search (GES) (Chickering, 2003), which performs a greedy search over the space of the Markov Equivalence Classes (MEC) of DAGs, i.e., a CPDAG. GES consists of two phases: a forward phase, where edges are added to the graph to maximize the score, and a backward phase, where edges are removed to further improve the score. The algorithm is guaranteed to return the correct equivalence class for $n \rightarrow \infty$ samples under the assumption of causal sufficiency, faithfulness, and in the presence of a consistent and decomposable scoring criterion (Chickering, 2003):

$$L(H, \mathbb{V}) = \sum_{i=1}^k l_i(V_i, Pa_i^H)$$

The Bayesian Information Criterion (BIC) is an example of a consistent and decomposable scoring criterion. On a practical level, undirected edges are accounted for in both possible directions of the arc; this will be key in the computation of the regret score of our method.

We can define the intersection operator over CPDAGs as follows:

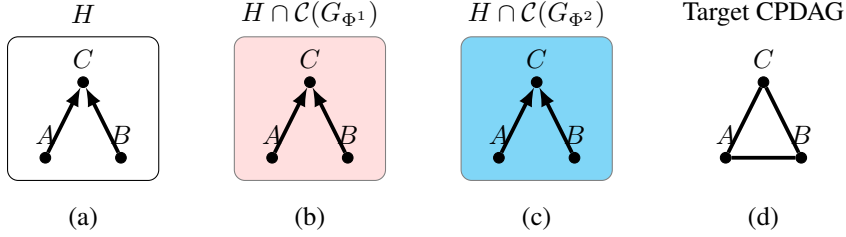


Figure 2: (a) Server PDAG obtained at an intermediate iteration (prior to convergence); (b) Intersection Server CPDAG and CPDAG client 1; (c) Intersection Server CPDAG and CPDAG client 2; (d) Target CPDAG result of the second phase of I-PERI.

Definition 2.3 (Intersection between Graphs). Given two CPDAGs, $G^k = (\mathbb{V}, \mathbb{E}^k)$ and $G^l = (\mathbb{V}, \mathbb{E}^l)$, the intersection between the two graphs is defined as follows:

$$G^k \cap G^l = (\mathbb{V}, \mathbb{E}^k \cap \mathbb{E}^l)$$

Where the operator \cap is defined as follows:

- if $V_i \multimap V_j \in \mathbb{E}^k$ and $V_i \multimap V_j \in \mathbb{E}^l$, then $V_i \multimap V_j \in \mathbb{E}^k \cap \mathbb{E}^l$
- if $V_i \not\multimap V_j$ in either \mathbb{E}^k or \mathbb{E}^l , then $V_i \not\multimap V_j$ in $\mathbb{E}^k \cap \mathbb{E}^l$
- if $V_i \rightarrow V_j \in \mathbb{E}^k$ and $V_i \rightarrow V_j \in \mathbb{E}^l$, then $V_i \rightarrow V_j \in \mathbb{E}^k \cap \mathbb{E}^l$
- if $V_i \rightarrow V_j \in \mathbb{E}^k$ and $V_i \rightarrow V_j \in \mathbb{E}^l$, then $V_i \rightarrow V_j \in \mathbb{E}^k \cap \mathbb{E}^l$

where \multimap denotes an undirected edge, \rightarrow , or a directed one, \rightarrow .

The intersection between graphs (Definition 2.3) subsumes a new definition of inclusion, in which a directed edge between two vertices, $V_i \rightarrow V_j$, is always included in an undirected one, $V_i \rightarrow V_j$.

Definition 2.4 (Inclusion between Graphs). Given two CPDAGs, $G^k = (\mathbb{V}, \mathbb{E}_k)$ and $G^l = (\mathbb{V}, \mathbb{E}_l)$, we say that $G^k \subseteq G^l$ if for all $V_i \rightarrow V_j \in \mathbb{E}_k$ exists an edge between V_i and V_j in G^l such that $V_i \rightarrow V_j \in \mathbb{E}^k$ or $V_i \rightarrow V_j \in \mathbb{E}^l$.

Regret-based Federated Causal Discovery Regret-based Federated Causal Discovery aims, as formulated in Mian et al. (2022, 2023), to discover causal structure while sharing only regrets, thereby preserving privacy at the client level. In this framework, regrets quantify the discrepancy between a candidate global graph and the local graph discovered at the client level. At every moment, the server shares the reconstructed global graph and computes a regret for each client based on a consistent scoring function.

Definition 2.5 (Regret). Let \mathbb{D}^k be the dataset at the client-level, H a candidate global graph, $\mathcal{C}(G)$ the client CPDAG, and L a consistent scoring function. We can define the regret function over H and $\mathcal{C}(G)$ as follows:

$$R_k(H) = L(H, \mathbb{D}^k) - L(\mathcal{C}(G), \mathbb{D}^k). \quad (1)$$

$R_k(H)$ is minimal when $L(H, \mathbb{D}^k)$ and $L(\mathcal{C}(G), \mathbb{D}^k)$ are equal, meaning H and $\mathcal{C}(G)$ are identical.

The algorithm in Mian et al. (2023), called PERI, finds the CPDAG minimizing the worst regret across clients, i.e.:

$$\hat{G} = \arg \min_{H \in \mathbb{G}} \max_k R_k(H). \quad (2)$$

This operation is performed iteratively following the GES algorithm, adding and removing edges accordingly to minimize the worst regret across clients. The GES algorithm is also applied locally at the client level to approximate the local CPDAG. In the setting of the PERI algorithm, it is assumed that all data at the client level are sampled from the same observational distribution, and that the underlying causal graph is identical across all clients and not subject to interventions. The graph minimizing the worst regret, \hat{G} , will be the graph such that $\hat{G} = \mathcal{C}(G)$ for every client k .

This paper extends the PERI algorithm in three directions to: (i) handle interventional data at the client-level with unknown targets; (ii) identify a tighter equivalence class, namely Φ -Markov Equivalence Class (Φ -MEC); (iii) allow the use of any causal discovery algorithm at the client level that returns a DAG or a CPDAG (e.g. PC).

3 Regret-Based Federated Causal Discovery with Unknown Interventions

The intuition behind Intervention-PERI (or I-PERI), is that the intervened graph at the client-level can have missing edges —i.e., edges removed due to structural interventions. Thus, the best we can recover at the client level is the CPDAG of the mutilated graph, $\mathcal{C}(G_{\Phi^k})$. This hinders the capability of PERI to recover the true CPDAG at the server-level, since the regret function as defined in Equation (1) would never converge in this setting. Additionally, intervening on the parents of a shielded collider can generate new v-structures, as shown in Figure 3 (d), meaning that the client CPDAG may provide additional information about edge orientations. To this end, I-PERI overcomes this issues in two steps:

1. First, it recovers, \hat{G} , which corresponds to the CPDAG $\mathcal{C}(G)$ and contains all client CPDAGs, ie., $\mathcal{C}(G_{\Phi^k}) \subseteq \hat{G}$, as per Definition 2.4.
2. Further orients edges in \hat{G} based on v-structures present at the client-level due to structural interventions, yielding a more refined equivalence class.

3.1 Federated CPDAG Aggregation

The first step of I-PERI identifies a CPDAG at the server-level that include all client CPDAGs. Since the client graphs can be a mutilated graph of the true causal DAG, directly applying the regret function as defined in Equation (1) would not converge. To address this issue, we propose to compute the regret function over the intersection graph between the server graph and each client graph. The intuition is that the regret function can be minimal even in case of missing edges in the client graphs, but will penalize an edges missing in the global graph and present in the client graph. Ultimately, the scoring function will be minimal when the client graph is a subgraph of the server one. The intersection graph between the server and the k -th client graph, denoted $\hat{G} \cap \mathcal{C}(G_{\Phi^k})$, as defined in Definition 2.3, will be equal to the client graph when the global graph converges to the true CPDAG, $\hat{G} \cap \mathcal{C}(G_{\Phi^k}) = \mathcal{C}(G_{\Phi^k})$.

Example 3.1. Let us consider the scenario in Figure 1, where client 1 contains observational data. Assuming to have an approximate CPDAG, \hat{G} , at the server-level as in Figure 2, we can compute the regret for each node as shown in Table 1.

The regret function can be rewritten as:

$$R_k(H) = L(H \cap \mathcal{C}(G_{\Phi^k}), \mathbb{D}^k) - L(\mathcal{C}(G_{\Phi^k}), \mathbb{D}^k) \quad (3)$$

Incorporating Equation (3) into the optimization problem of Equation (2) allows the discovery of a representative of the MEC of the true causal DAG, for which all client-level DAGs are subgraphs.

Theorem 3.2. *Let G denote the true server causal DAG, and let $\mathcal{C}(G)$ denote its corresponding CPDAG. Let Φ denote the family of unknown intervention targets across the K clients. For each client $k \in \{1, \dots, K\}$, let G_{Φ^k} denote the client-specific causal DAG. Let \hat{G} be defined as the graph approximated by solving Equation (3) using the regret function as defined in Equation (2). If at the client level, the CPDAG $\mathcal{C}(G_{\Phi^k})$ of each G_{Φ^k} is known to client k , if L is a consistent scoring function, and if Assumption 2.1 holds, then \hat{G} converges to $\mathcal{C}(G)$.*

We emphasize that causal sufficiency and faithfulness are not explicitly assumed in the statement of the theorem, since the client-level CPDAGs are assumed to be available. When this assumption does not hold, each client CPDAG can be estimated from data under the standard assumptions of causal sufficiency and faithfulness using classical causal discovery methods, such as the PC (Spirtes et al., 2001) or GES (Chickering, 2003) algorithms.

3.2 Orientation Refinement

In presence of structural interventions, additional v-structures may become identifiable, as shown in Figure 3 (d). A structural intervention transforming a shielded collider into an unshielded one enables orienting the corresponding edges in the server graph. The second phase of I-PERI refines the orientation of ambiguous (i.e., undirected) edges in the global CPDAG. To this end, we penalize edges that are unoriented in the aggregate CPDAG but are oriented in a client graph. This is achieved computing the regret over the intersection between the server graph and the skeleton of the client graph, $\hat{G} \cap \text{Skel}(G_{\Phi^k})$.

Example 3.3. Let us consider the scenario in Figure 1, where client 2 contains interventional data that allow to orient a v-structure. Assuming to have an approximate PDAG, H , at the server-level as in Figure 3, we can compute the regret for each node as shown in Table 1.

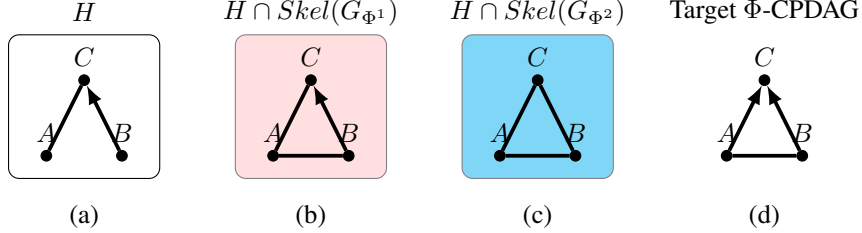


Figure 3: (a) Server PDAG obtained at an intermediate iteration (prior to convergence); (b) Intersection Server CPDAG and skeleton of client 1 CPDAG; (c) Intersection Server CPDAG and skeleton of client 2 CPDAG; (d) target Φ -CPDAG result of the second phase of I-PERI.

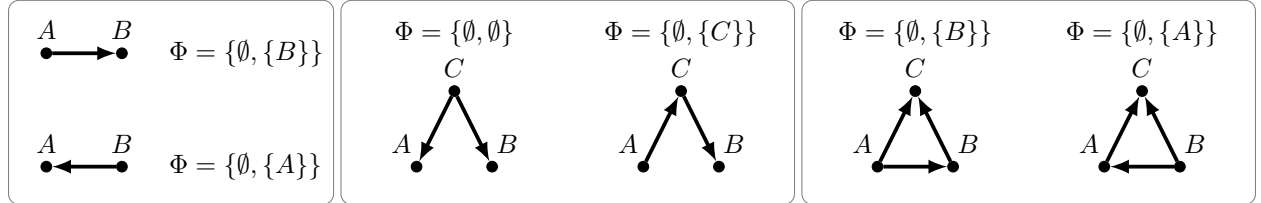


Figure 4: Three sets of server DAGs with their associated intervention targets where each set contains server DAGs that are Φ -Markov equivalent.

Intersecting with the skeleton removes any edge that has been structurally intervened upon at the client level, thereby allowing us to penalize edges that are unoriented at the server level but directed at the client level. Since the regret function is based on a consistent and decomposable scoring function, it accounts for both possible orientations of undirected edges. Minimizing the regret requires orienting edges in the server graph according to the client graph. If no additional orientations can be inferred, the regret will not decrease further, and the server graph will remain unchanged. We can thus rewrite Equation (1) as:

$$R_k(H) = L(H \cap \text{Skel}(G_{\Phi^k}), \mathbb{D}^k) - L(\mathcal{C}(G_{\Phi^k}), \mathbb{D}^k) \quad (4)$$

The optimization problem remains the same as in Equation (2), but the search space is now limited to PDAGs derived from the server CPDAG by orienting undirected edges.

Φ-Markov Equivalence Class. The second step I-PERI allows us to identify a tighter equivalence class than the observational MEC. Let us consider a family of unknown interventions across K clients, Φ , observed only locally in a federated setting. We can then define the Φ -Markov Equivalence Class as follows:

Definition 3.1 (Φ -Markov Equivalence). Given two server graphs and relative intervention targets families, $\langle G^1, \Phi_1 \rangle$ and $\langle G^2, \Phi_2 \rangle$, we say that G^1 and G^2 are Φ -Markov equivalent, denoted as $G^1 \sim_{\Phi} G^2$, if and only if, for every disjoint sets $\mathbb{X}, \mathbb{Y}, \mathbb{Z} \subset \mathbb{V}$:

$$\mathbb{X} \perp\!\!\!\perp_{G^1} \mathbb{Y} | \mathbb{Z} \Leftrightarrow \mathbb{X} \perp\!\!\!\perp_{G^2} \mathbb{Y} | \mathbb{Z}$$

and:

$$\begin{aligned} \exists \Phi_1^k \in \Phi_1, \quad \exists W \in \mathbb{V} \setminus \mathbb{X} \cup \mathbb{Y} \cup \mathbb{Z}, \quad (\mathbb{X} \perp\!\!\!\perp_{G_{\Phi_1^k}} \mathbb{Y} | \mathbb{Z} \wedge \mathbb{X} \not\perp\!\!\!\perp_{G_{\Phi_1^k}} \mathbb{Y} | \mathbb{Z}, W) \Leftrightarrow \\ \exists \Phi_2^l \in \Phi_2, \quad \exists W \in \mathbb{V} \setminus \mathbb{X} \cup \mathbb{Y} \cup \mathbb{Z}, \quad (\mathbb{X} \perp\!\!\!\perp_{G_{\Phi_2^l}} \mathbb{Y} | \mathbb{Z} \wedge \mathbb{X} \not\perp\!\!\!\perp_{G_{\Phi_2^l}} \mathbb{Y} | \mathbb{Z}, W). \end{aligned}$$

It is important to note that the sets Φ_1^k and Φ_2^l appearing in the definition are not required to correspond to the same intervention targets. For illustration, Figure 4 presents three sets of graphs, each consisting of graphs that are Markov equivalent. Notably, within each class, the graphs are associated with different intervention target sets, despite being Markov equivalent. Moreover, the definition does not require that a mutilated graph relative to Φ_1 to have a mutilated graph relative to Φ_2 with a same skeleton. For illustration, see Figure 5 which shows two server DAGs that are Φ -Markov equivalent but some of their mutilated graphs do not share the same skeleton.

In the following, we show that all graphs that are Markov equivalent can be characterized graphically.

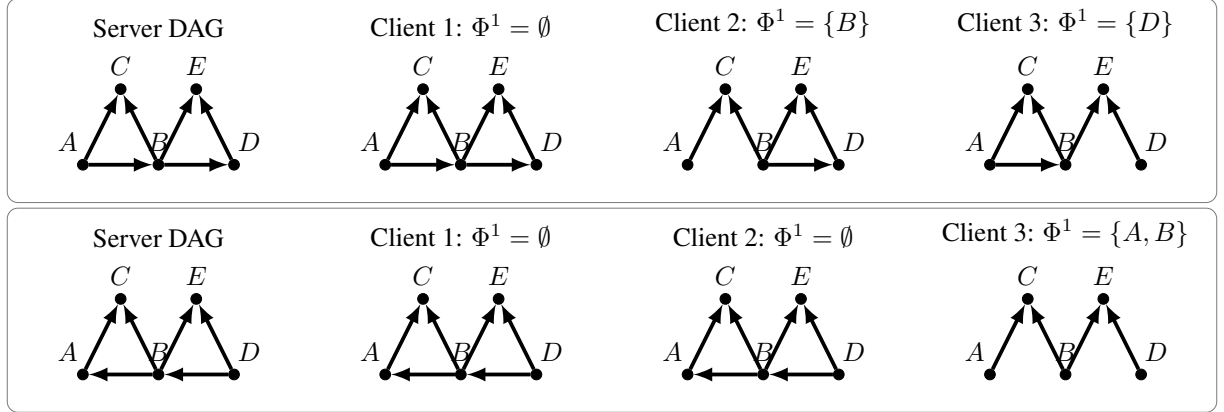


Figure 5: Example showing that, for two server-level DAGs that are Φ -Markov equivalent, the corresponding skeleton of client-level mutilated graphs are not necessarily identical.

Theorem 3.4 (Characterization of Φ -Markov Equivalence Class). *Two server graphs G^1 and G^2 with unknown intervention targets families Φ^1 and Φ^2 belong to the same Φ -Markov equivalence class (Φ -MEC) if and only if:*

1. G^1 and G^2 have the same skeleton
2. G^1 and G^2 have the same v-structures
3. There exists $\Phi_1^k \in \Phi^1$ such that a v-structure appears in $G_{\Phi_1^k}^1$ that is not present in G^1 if and only if there exists $\Phi_2^l \in \Phi^2$ such that the same v-structure appears in $G_{\Phi_2^l}^2$ and is not present in G^2 .

We now define the representative of a Φ -MEC, denoted as Φ -CPDAG, which is obtained from CPDAG, by orienting some undirected edges while keeping the skeleton fixed.

Definition 3.2 (Φ -CPDAG). Let G be a server causal DAG and Φ a set of intervention targets over multiple clients. Let us define the CPDAG of G as $\mathcal{C}(G)$. The partially directed graph obtained by orienting in $\mathcal{C}(G)$ every v-structure in the intervened graph G_{Φ^k} for every $\Phi^k \in \Phi$ is called the Φ -CPDAG of G . We will denote such graph as $\Phi(G)$.

Given a Φ -Markov equivalence class, the Φ -CPDAG for that class is unique. We emphasize this result with a corollary.

Corollary 3.1. *Let $\Phi_1(G^1)$ and $\Phi_2(G^2)$ be the Φ -CPDAGs of two causal DAGs G^1 and G^2 and Φ^1 and Φ^2 two intervention families with unknown targets. If $G^1 \sim_{\Phi} G^2$, then $\Phi_1(G^1) = \Phi_2(G^2)$.*

We can now show that I-PERI converges to the Φ -CPDAG of the true causal DAG.

Theorem 3.5 (Correctness of I-PERI). *Let G denote the true server causal DAG, and let $\mathcal{C}(G)$ denote its corresponding CPDAG. Let Φ denote the family of unknown intervention targets across the K clients. For each client $k \in \{1, \dots, K\}$, let G_{ϕ^k} denote the client-specific causal DAG. Let \hat{G} be the output of I-PERI. If at the client level, the CPDAG $\mathcal{C}(G_{\phi^k})$ of each G_{ϕ^k} is known to client k , if L is a consistent scoring function, and if Assumption 2.1 holds, then \hat{G} converges to $\Phi(G)$.*

As in the case of Theorem 3.2, causal sufficiency and faithfulness are not stated explicitly in Theorem 3.5, as the result is formulated under the premise that the client-level CPDAGs are available. When these are unknown, they can be estimated using PC or GES under the omitted assumptions.

3.3 Privacy Guarantees

Sharing regrets among clients and server intuitively reveals less information than sharing the local graph or model parameters. However, we should account for the fact that sharing the global causal graph may violate privacy requirements, even though this can be accounted for using basic encryption methods. Additionally, we could reconstruct the local causal graph based on the shared regrets and the global graph using Equation (2). This would allow to identify interventions at the client-level, however, this problem is NP-hard (Chickering et al., 2004).

As for PERI, we can prove that I-PERI is differentially private by bounding the sensitivity of the regret function. A given algorithm \mathcal{A} is ϵ -differentially private if, for any two datasets \mathbb{D} and \mathbb{D}' that differ in at most one record, for any

CPDAG Aggregation			
Node	$H \cap \mathcal{C}(G^1)$	$\mathcal{C}(G^1)$	Regret
	Parents		
A	{}	{B,C}	$R > 0$
B	{}	{A,C}	$R > 0$
C	{A,B}	{A,B}	$R = 0$
Orientation Refinement			
Node	$H \cap \text{Skle}(G^2)$	$\mathcal{C}(G^2)$	Regret
	Parents		
A	{C}	{}	$R > 0$
B	{}	{}	$R = 0$
C	{A,B}	{A,B}	$R = 0$

Table 1: Regret computation for each node comparing the server CPDAG and client 1 CPDAG.

output set \mathbb{O} :

$$P(\mathcal{A}(\mathbb{D}) \in \mathbb{O}) \leq e^\epsilon P(\mathcal{A}(\mathbb{D}') \in \mathbb{O})$$

where ϵ is the privacy loss, i.e., for smaller values of ϵ we have stronger privacy. The idea is that injecting noise to the regret function will prevent an attacker from inferring the presence of a specific record in the local dataset. To do so, we need to show that the sensitivity of the regret function is bounded, namely, how much the regret function changes when a single record in the dataset is changed. Let us consider that each graph at the local level, G^k , is described by a set of parameters ϕ^k . Assuming to have a consistent scoring function L , if we have a dataset \mathbb{D}^k and a dataset \mathbb{D}'^k that differ in a single record, we have that $\|\phi^k - \phi'^k\| \propto \frac{1}{n}$ (Mian et al., 2023).

Lemma 3.1. *Assume $P^k(x; \theta)$ to be uniformly lower-bounded by r , namely, $\forall x \in \mathbb{D} \forall \theta \in \Theta : P_k(x, \theta) \geq r$, that $\|\theta\| \leq M$ for all model parameters $\theta \in \Theta$ and that the score L is partially differentiable with respect to θ . Let \mathbb{D}_k and \mathbb{D}'_k be datasets that differ in a single element, $\mathbb{D}_k \setminus \mathbb{D}'_k = x_i$, and that θ and θ' are the respective local parameters, with respective regrets $\hat{R}_k(G)$ and $\hat{R}'_k(G)$. We assume that $\|\theta - \theta'\| \leq \frac{2M}{n}$. Then the sensitivity of the regret function is bounded by:*

$$\max | \hat{R}_i(G) - \hat{R}'_i(G) | \leq (2M + 1) \log r^2 + \mathcal{O}\left(\frac{\log n}{n}\right).$$

Proposition 3.1. *Assume each local regret \hat{R}_k has sensitivity $\leq Q$, then I-PERI with i.i.d. Laplace noise with scale $\lambda = \frac{Q}{\epsilon}$ added to each \hat{R}_k is ϵ -differentially private.*

4 Experiments

We evaluated I-PERI on synthetic data designed to mimic different scenarios with varying amount of samples, variables and clients. Results are reported in Figure 6.

Synthetic Data. The true DAGs are generated following the Erdos-Renyi model Erdös & Rényi (1960), with an expected number of edges equal to the number of nodes. Each client dataset is generated according to a linear SEM with additive Gaussian noise of the form:

$$X_i = \sum_{X_j \in Pa_i^G} w_{ji} X_j + N_i \quad (5)$$

where the noise $N_i \sim \mathcal{N}(0, 1)$ and the edge weights w_{ji} are sampled uniformly at random from the union of the intervals $[-1, -0.1]$ and $[0.1, 1]$ to avoid values close to zero. Moreover, to highlight the improvements introduced by I-PERI in the second phase orienting additional edges on the union CPDAG, we artificially introduce shielded colliders prioritizing interventions at the client level creating v-structures that would not identifiable from purely observational data.

Metrics. We evaluate the performance of I-PERI using two metrics:

- **Structural Hamming Distance (SHD):** measures the number of edge additions, deletions, or reversals required to transform the learned graph into the true graph.
- **F1-score:** which assess the accuracy of the edge orientation in the estimated DAG.

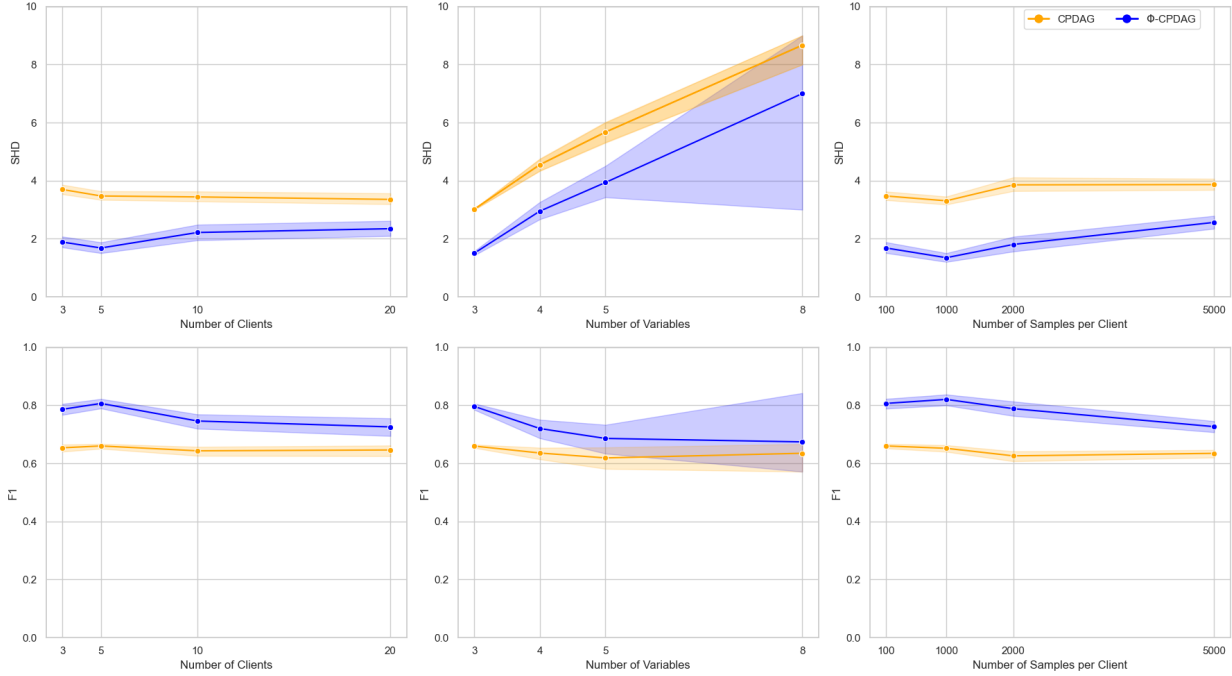


Figure 6: Comparison SHD and F1 error over the estimated CPDAG (orange) and the estimated Φ -CPDAG (blue) against the true DAG using I-PERI. The first and second column present results with sample heterogeneity, namely $n_k \in \{1000, 2000, 5000\}$, while the second and third column are relative to experiment with $K = 5$.

Results. The results reported in Figure 6 corroborate the effectiveness of I-PERI in orienting additional edges beyond those identified in the CPDAG. Experiments varying the number of samples or variables are conducted in a setting with 5 clients. In contrast, experiments that vary the number of clients and variables assume heterogeneous sample sizes across clients, specifically 1000, 2000, or 5000 samples per client. Overall, the estimated Φ -CPDAG consistently achieves lower SHD and higher F1-score than the CPDAG when compared to the true DAG.

5 Discussion

This work addresses a key limitation of existing federated causal discovery methods by relaxing the common assumption that all clients share an identical causal model and experience no interventions. By explicitly accounting for unknown client-level interventions, our approach better reflects the heterogeneity encountered in real-world federated environments, such as multi-center clinical studies or distributed organizational data systems.

A central insight of this paper is that client heterogeneity induced by interventions can be leveraged rather than ignored. While such heterogeneity is often viewed as a complication in federated learning, I-PERI exploits intervention-induced structural differences across clients to orient additional edges beyond what is identifiable from purely observational data. This results in a strictly tighter equivalence class, captured by the proposed Φ -Markov Equivalence Class. Furthermore, I-PERI enforces privacy by design, through restricted information sharing and server-side aggregation. This bottom-up approach offers a favorable trade-off between privacy, computational efficiency, and statistical power, though it may not provide the same formal guarantees as cryptographic methods in adversarial settings.

In the main body of this work, we focused on structural interventions, as they represent the most challenging and informative setting for federated causal discovery. Nevertheless, I-PERI is also sound in the absence of structural interventions, including settings with purely observational data or parametric interventions only. When client data contain exclusively parametric interventions or no interventions at all, I-PERI reduces to recovering the CPDAG of the union of the client DAGs. In this case, parametric interventions and purely observational data are treated equivalently by the algorithm, as they do not alter the underlying causal structure. Consequently, no additional edge orientations beyond those identifiable from observational data can be inferred at the server level. The intuition is straightforward. If one client observes purely observational data while another client applies a parametric intervention, both datasets are generated from the same causal DAG, differing only in the functional parameters or noise distributions. As a result,

each client can locally identify the same equivalence class, and aggregating this information at the server level yields the standard CPDAG of the union graph, without further refinement.

It is important to emphasize that this work differs from existing approaches to causal discovery with interventional data. For instance Hauser & Bühlmann (2012); Yang et al. (2018) assume that interventions are known, including explicit knowledge of which variables are intervened upon. Such assumptions substantially simplify the discovery problem but are often unrealistic in practical federated settings. In contrast, we consider a setting in which interventions are unknown to the server and may differ across clients. More recently, Jaber et al. (2020); Li et al. (2023); Squires et al. (2020); Wang et al. (2022) has established important results for causal discovery from datasets with unknown interventions. However, their setting assumes that all datasets can be pooled centrally, allowing direct comparison across intervention regimes. This centralized access enables stronger identifiability results than those attainable in a federated environment. In our setting, data from different clients cannot be pooled due to privacy constraints, and only limited information can be shared with the server. As a result, the server cannot directly compare distributions across intervention regimes. This restriction fundamentally alters the results and leads to a looser equivalence class than the one introduced in centralized settings with unknown interventions.

Despite these advantages, this work has several limitations. Our theoretical analysis relies on standard assumptions in causal discovery, including causal sufficiency (i.e., the absence of latent confounders), no selection bias and faithfulness. These assumptions may be violated in real-world settings. Extending the proposed framework to settings with latent variables, selection bias, or weaker assumptions remains an important direction for future research.

Acknowledgment

This work was supported by the CIPHOD project (ANR-23-CPJ1-0212-01).

References

Assaad, C. K., Devijver, E., and Gaussier, E. Survey and evaluation of causal discovery methods for time series. *J. Artif. Int. Res.*, 73, may 2022. ISSN 1076-9757. doi: 10.1613/jair.1.13428.

Chickering, D. M. Optimal structure identification with greedy search. *J. Mach. Learn. Res.*, 3(null):507–554, March 2003. ISSN 1532-4435. doi: 10.1162/153244303321897717.

Chickering, D. M., Heckerman, D., and Meek, C. Large-sample learning of bayesian networks is np-hard. *J. Mach. Learn. Res.*, 5:1287–1330, December 2004. ISSN 1532-4435.

Colombo, D. and Maathuis, M. H. Order-independent constraint-based causal structure learning. *J. Mach. Learn. Res.*, 15(1):3741–3782, January 2014. ISSN 1532-4435.

Erdős, P. and Rényi, A. On the evolution of random graphs. *Publ. Math. Inst. Hungar. Acad. Sci.*, 5:17–61, 1960.

Hauser, A. and Bühlmann, P. Characterization and greedy learning of interventional markov equivalence classes of directed acyclic graphs. *The Journal of Machine Learning Research*, 13(1):2409–2464, 2012.

Hernan, M. and Robins, J. *Causal Inference: What If*. Chapman & Hall/CRC Monographs on Statistics & Applied Probab. CRC Press, 2023. ISBN 9781420076165.

Jaber, A., Kocaoglu, M., Shanmugam, K., and Bareinboim, E. Causal discovery from soft interventions with unknown targets: Characterization and learning. In Larochelle, H., Ranzato, M., Hadsell, R., Balcan, M., and Lin, H. (eds.), *Advances in Neural Information Processing Systems*, volume 33, pp. 9551–9561. Curran Associates, Inc., 2020.

Kairouz, P., McMahan, H. B., Avent, B., Bellet, A., Bennis, M., Nitin Bhagoji, A., Bonawitz, K., Charles, Z., Cormode, G., Cummings, R., D’Oliveira, R. G. L., Eichner, H., El Rouayheb, S., Evans, D., Gardner, J., Garrett, Z., Gascón, A., Ghazi, B., Gibbons, P. B., Gruteser, M., Harchaoui, Z., He, C., He, L., Huo, Z., Hutchinson, B., Hsu, J., Jaggi, M., Javidi, T., Joshi, G., Khodak, M., Konecný, J., Korolova, A., Koushanfar, F., Koyejo, S., Lepoint, T., Liu, Y., Mittal, P., Mohri, M., Nock, R., Özgür, A., Pagh, R., Qi, H., Ramage, D., Raskar, R., Raykova, M., Song, D., Song, W., Stich, S. U., Sun, Z., Suresh, A. T., Tramèr, F., Vepakomma, P., Wang, J., Xiong, L., Xu, Z., Yang, Q., Yu, F. X., Yu, H., and Zhao, S. Advances and open problems in federated learning. *Found. Trends Mach. Learn.*, 14(1–2):1–210, June 2021. ISSN 1935-8237. doi: 10.1561/2200000083.

Li, A., Jaber, A., and Bareinboim, E. Causal discovery from observational and interventional data across multiple environments. In Oh, A., Naumann, T., Globerson, A., Saenko, K., Hardt, M., and Levine, S. (eds.), *Advances in Neural Information Processing Systems*, volume 36, pp. 16942–16956. Curran Associates, Inc., 2023.

Mian, O., Kaltenpoth, D., and Kamp, M. Regret-based federated causal discovery. In Le, T. D., Liu, L., Kıcıman, E., Triantafyllou, S., and Liu, H. (eds.), *Proceedings of The KDD’22 Workshop on Causal Discovery*, volume 185 of *Proceedings of Machine Learning Research*, pp. 61–69. PMLR, 15 Aug 2022.

Mian, O., Kaltenpoth, D., Kamp, M., and Vreeken, J. Nothing but regrets — privacy-preserving federated causal discovery. In Ruiz, F., Dy, J., and van de Meent, J.-W. (eds.), *Proceedings of The 26th International Conference on Artificial Intelligence and Statistics*, volume 206 of *Proceedings of Machine Learning Research*, pp. 8263–8278. PMLR, 25–27 Apr 2023.

Pearl, J. *Causality: Models, Reasoning and Inference*. Cambridge University Press, USA, 2nd edition, 2009. ISBN 052189560X.

Runge, J. Discovering contemporaneous and lagged causal relations in autocorrelated nonlinear time series datasets. In Peters, J. and Sontag, D. (eds.), *Proceedings of the 36th Conference on Uncertainty in Artificial Intelligence (UAI)*, volume 124 of *Proceedings of Machine Learning Research*, pp. 1388–1397. PMLR, 03–06 Aug 2020.

Spirites, P., Glymour, C., and Scheines, R. *Causation, prediction, and search*. MIT press, 2001.

Squires, C., Wang, Y., and Uhler, C. Permutation-based causal structure learning with unknown intervention targets. In Peters, J. and Sontag, D. (eds.), *Proceedings of the 36th Conference on Uncertainty in Artificial Intelligence (UAI)*, volume 124 of *Proceedings of Machine Learning Research*, pp. 1039–1048. PMLR, 03–06 Aug 2020.

Verma, T. and Pearl, J. Equivalence and synthesis of causal models. In *Proceedings of the Sixth Annual Conference on Uncertainty in Artificial Intelligence*, UAI '90, pp. 255–270, USA, 1990. Elsevier Science Inc. ISBN 0444892648.

Wang, Y., Cao, F., Yu, K., and Liang, J. Efficient causal structure learning from multiple interventional datasets with unknown targets. *Proceedings of the AAAI Conference on Artificial Intelligence*, 36(8):8584–8593, Jun. 2022. doi: 10.1609/aaai.v36i8.20836.

Yang, K., Katcoff, A., and Uhler, C. Characterizing and learning equivalence classes of causal DAGs under interventions. In Dy, J. and Krause, A. (eds.), *Proceedings of the 35th International Conference on Machine Learning*, volume 80 of *Proceedings of Machine Learning Research*, pp. 5541–5550. PMLR, 10–15 Jul 2018.

Theorem 3.2. *Let G denote the true server causal DAG, and let $\mathcal{C}(G)$ denote its corresponding CPDAG. Let Φ denote the family of unknown intervention targets across the K clients. For each client $k \in \{1, \dots, K\}$, let G_{ϕ^k} denote the client-specific causal DAG. Let \hat{G} be defined as the graph approximated by solving Equation (3) using the regret function as defined in Equation (2). If at the client level, the CPDAG $\mathcal{C}(G_{\phi^k})$ of each G_{ϕ^k} is known to client k , if L is a consistent scoring function, and if Assumption 2.1 holds, then \hat{G} converges to $\mathcal{C}(G)$.*

Proof. By Corollary 3 of Mian et al. (2023), if clients contain only observational data, minimizing the worst-case regret recovers the true graph asymptotically. In the general case with interventions, the intersection-based regret $R_k(\hat{G})$, defined as per Equation (3), is minimized when the candidate global graph \hat{G} contains all edges present in client k , i.e., when $\subseteq \hat{G}$, as per Definition 2.4. Hence, any global graph \hat{G} that minimizes the worst-case regret across all clients must satisfy

$$\bigcup_{k=1}^K \mathcal{C}(G_{\phi^k}) = \hat{G}.$$

where $\hat{\mathbb{E}} = \bigcup_{k=1}^K \mathbb{E}^k$. We assume that all client graphs are derived from the same true graph G , thus $\mathcal{C}(G_{\phi^k}) \subseteq \mathcal{C}(G)$, and Assumption 2.1 ensures that at least one purely observational client allows consistent identification of edge orientations. Combining these facts, no edge of $\mathcal{C}(G)$ can be missing in \hat{G} , and no orientation can be misidentified asymptotically. Therefore, \hat{G} converges to the true CPDAG $\mathcal{C}(G)$ as the sample sizes grow. \square

Theorem 3.4 (Characterization of Φ -Markov Equivalence Class). *Two server graphs G^1 and G^2 with unknown intervention targets families Φ^1 and Φ^2 belong to the same Φ -Markov equivalence class (Φ -MEC) if and only if:*

1. G^1 and G^2 have the same skeleton
2. G^1 and G^2 have the same v-structures
3. There exists $\Phi_1^k \in \Phi^1$ such that a v-structure appears in $G_{\Phi_1^k}^1$ that is not present in G^1 if and only if there exists $\Phi_2^l \in \Phi^2$ such that the same v-structure appears in $G_{\Phi_2^l}^2$ and is not present in G^2 .

Proof. (\Rightarrow) If $G_1 \sim_{\Phi} G_2$ by Definition 3.1 they imply the same observational d -separations. Hence, they have the same skeleton and v-structures (Verma & Pearl, 1990). Moreover, as per Definition 3.1, two graphs are in the same Φ -MEC if, when an intervention set exposes a new v-structure in one graph, $G_{\Phi_1^k}$, there exist at least another intervention set that generates the same v-structure in the second one, $G_{\Phi_2^l}$, and vice-versa.

(\Leftarrow) If the two graphs have the same skeleton and v-structures, they are in the same MEC. If $G_{\Phi_1^k}$ and $G_{\Phi_2^l}$ share the same v-structure, there exist $\mathbb{X}, \mathbb{Y}, \mathbb{Z} \subset \mathbb{V}$ and $W \in \mathbb{V} \setminus \mathbb{X} \cup \mathbb{Y} \cup \mathbb{Z}$ such that when conditioning on \mathbb{Z} and W creates the same conditional dependence in both graphs. Hence, by Definition 3.1, $G_1 \sim_{\Phi} G_2$. \square

Corollary 3.1. *Let $\Phi_1(G^1)$ and $\Phi_2(G^2)$ be the Φ -CPDAGs of two causal DAGs G^1 and G^2 and Φ^1 and Φ^2 two intervention families with unknown targets. If $G^1 \sim_{\Phi} G^2$, then $\Phi_1(G^1) = \Phi_2(G^2)$.*

Proof. From Theorem 3.4 and Definition 3.2 \square

Theorem 3.5 (Correctness of I-PERI). *Let G denote the true server causal DAG, and let $\mathcal{C}(G)$ denote its corresponding CPDAG. Let Φ denote the family of unknown intervention targets across the K clients. For each client $k \in \{1, \dots, K\}$, let G_{ϕ^k} denote the client-specific causal DAG. Let \hat{G} be the output of I-PERI. If at the client level, the CPDAG $\mathcal{C}(G_{\phi^k})$ of each G_{ϕ^k} is known to client k , if L is a consistent scoring function, and if Assumption 2.1 holds, then \hat{G} converges to $\Phi(G)$.*

Proof. From Theorem 3.2, I-PERI converges to the CPDAG \hat{G} such that every client graph, $\mathcal{C}(G_{\phi^k})$, is a subgraph of \hat{G} , $\mathcal{C}(G_{\phi^k}) \subseteq \hat{G}$. If we define $R_k(\hat{G})$ using Equation (4), then $R_k(\hat{G}) = 0$ if all edges oriented in $\mathcal{C}(G_{\phi^k})$ are oriented in \hat{G} for every $\Phi^k \in \Phi$. Meaning that for every G^m , and for all $V_i \in \mathbb{V}$,

$$L(V_i, Pa_{G_{\phi^k}}(V_i); \mathbb{D}^k) = L(V_i, Pa_{\hat{G} \cup Skel(G_{\phi^k})}(V_i); \mathbb{D}^m)$$

Meaning that $Pa_{G_{\phi^k}}(V_i) = Pa_{\hat{G} \cup Skel(G_{\phi^k})}(V_i)$. Thus regret is minimal only if \hat{G} is the Φ -CPDAG of the true graph G . \square

Lemma 3.1. Assume $P^k(x; \theta)$ to be uniformly lower-bounded by r , namely, $\forall x \in \mathbb{D} \ \forall \theta \in \Theta : P_k(x, \theta) \geq r$, that $\|\theta\| \leq M$ for all model parameters $\theta \in \Theta$ and that the score L is partially differentiable with respect to θ . Let \mathbb{D}_k and \mathbb{D}'_k be datasets that differ in a single element, $\mathbb{D}_k \setminus \mathbb{D}'_k = x_i$, and that θ and θ' are the respective local parameters, with respective regrets $\hat{R}_k(G)$ and $\hat{R}'_k(G)$. We assume that $\|\theta - \theta'\| \leq \frac{2M}{n}$. Then the sensitivity of the regret function is bounded by:

$$\max |\hat{R}_k(G) - \hat{R}'_k(G)| \leq (2M + 1) \log r^2 + \mathcal{O}\left(\frac{\log n}{n}\right).$$

Proof. Follows from Lemma 4 of Mian et al. (2023). \square

Proposition 3.1. Assume each local regret \hat{R}_k has sensitivity $\leq Q$, then I-PERI with i.i.d. Laplace noise with scale $\lambda = \frac{Q}{\epsilon}$ added to each \hat{R}_k is ϵ -differentially private.

Proof. Follows from Lemma 3.1 and Proposition 5 of Mian et al. (2023). \square